MICROSCOPIC STUDY OF MULTIFUNCTIONAL DRUG MOLECULE ADHESION TO ELECTRONIC BIOSENSORS COATED WITH DIAMOND AND GOLD NANOPARTICLES

[1]Tomáš FINSTERLE, [1]Ivana PILARČÍKOVÁ, [1]Ilona ALI BLÁHOVÁ, [2]Štěpán POTOCKÝ, [2]Alexander KROMKA, [2]Egor UKRAINTSEV, [3]Eugenie NEPOVIMOVÁ, [3]Kamil MUSÍLEK, [3]Kamil KUČA, [1]Bohuslav REZEK

[1]Faculty of Electrical Engineering, Czech Technical University in Prague, Czech Republic, EU
finsttom@fel.cvut.cz
[2]Institute of Physics, Czech Academy of Sciences, Prague, Czech Republic, EU
[3]Faculty of Science, University of Hradec Kralove, Czech Republic, EU

Abstract

The easy and fast detection of drug content and concentration levels is demanded in biological research as well as in clinical practice. Here we study on microscopic level how nanodiamonds and gold nanoparticles interact with a multifunctional drug molecule directly on a biosensor surface. The sensors are made of interdigitated Au electrodes coated by 5 nm hydrogenated or oxidized nanodiamonds and further combined with Au colloidal nanoparticles (size 20 nm) providing nanoscale composite (spacing 100 nm). Atomic force microscopy is employed to measure local tip-surface adhesion forces and surface topography. AFM adhesion maps show that the drug binds to all types of nanoparticles and the adhesion is also significantly influenced by the substrates on which the nanoparticles are deposited. Role of local AFM tip interaction with nanostructured surface is also discussed.

Keywords: Biosensors, nanoparticles, nanodiamonds, Alzheimer drugs

1. INTRODUCTION

The easy and fast detection of drug content and concentration levels is demanded in biological research as well as in clinical practice. Therefore, label-free platforms based on electrical detection are intensively developed. Nanomaterials and structures are often introduced to provide a fast and sensitive response. [1] Nanodiamonds have unique properties for use in biosensors.[2] Nanocrystalline diamond provides a convenient combination of physical, mechanical, chemical, biocompatible and electrical properties [3-5]. Based on analysis using SEM and AFM microscopy we study on microscopic level how nanodiamonds and gold nanoparticles interact with drug molecules. As a model system we use experimental multifunctional molecule for treatment of Alzheimer disease [6].

2. MATERIALS AND METHODS

For the preparation of sensors, commonly available sensors were used. Gold interdigital electrodes (IDE) are sputtered on the ceramic substrate (15-50 um gap, overall size 5 × 6 mm^2) coated by nanodiamonds. Suspensions of detonation nanodiamond particles (hydrogenated H-DND and air-annealed O-DND) were prepared by ultrasonication and centrifugation in water and then drop casted (10 uL) on the active sensor area. Both types of sensors were also further combined with Au colloidal nanoparticles (AuNP, size 20 nm) for providing nanoscale binding sites. For drug binding were then functionalized in MTAB (myristyltrimethylammonium bromide) and finally exposed to 1-EN-142 drug [6] in DMSO (10 % solution) and rinsed by water and methanol to remove all excess residues.

The electrode system allows the measurement of various sensitive layers. The used sensor consists of a layer structure with different roughness. The reason for using this sensor is that it is a commonly available platform.

The nanodiamond layer itself has different properties when it comes to O-DND or H-DND. Their properties are also strongly affected depending on the substrate used [7].

A set of sensor samples with different combinations of applied coatings (H-DND, MTAB, Au nanoparticles, drug 1-EN-142) were examined. Suspensions of detonation nanodiamond (DND) particles based on hydrogenated H-DND (as received, polyfunctional, positive zeta potential) and air-annealed O-DND (purified and oxidized by annealing in air at 450 °C, 30 min, negative zeta potential) were prepared by ultrasonication and centrifugation in water (20 mg of powder in 1 mL). Then 1 mL of supernatant was carefully extracted by a micropipette and diluted 10× by demi water prior to further use. Gold nanoparticles (AuNP) were obtained from a colloidal solution of citrate stabilized 20 nm Au particles (BBI Solutions, EM.GC 20, 0.06 wt%, particle density of 7×10^{11} particles per 1 mL).

The morphological differences of the prepared sensors were studied by scanning electron microscopy (SEM) using Tescan MAIA 3 in secondary electron mode. Atomic force microscopy (Bruker ICON, CF4 treated Multi75AL cantilevers) was employed to measure local tip-surface adhesion forces and surface topography. Characteristic sensor area of 1×1 um^2 was examined at a scan rate of 0.1 Hz and resolution of 512x512 pixels. Plane correction and correction of scars were applied on adhesion images using Gwyddion software [8,9] to improve the visibility of the features. Tip particle adhesion on individual particles were evaluated also Gwyddion program. The basic principle was to determine adhesions of the small area typical 20×20 nm^2 on individual particles. This area was always selected at the top of the particle. Determining adhesion from the area and not from the single top point on the particle allowed us to reduce the RMS of the adhesion signal.

3. RESULTS AND DISCUSSION

Figure 1a shows the schematic drawing of the sensor coated with DND and Au nanoparticles. **Figure 1b** shows typical SEM microscopic morphology of the sensor surface, in this case coated with O-DND/AuNP composite and with the adsorbed drug (EN). Fine nanostructured morphology is observed all over the electrode surface. This indicates dense coating of the electrodes by O-DND nanodiamonds. In addition, there are bright points noticeable. They most likely correspond to AuNP. This assumption is confirmed by further AFM adhesion analysis.

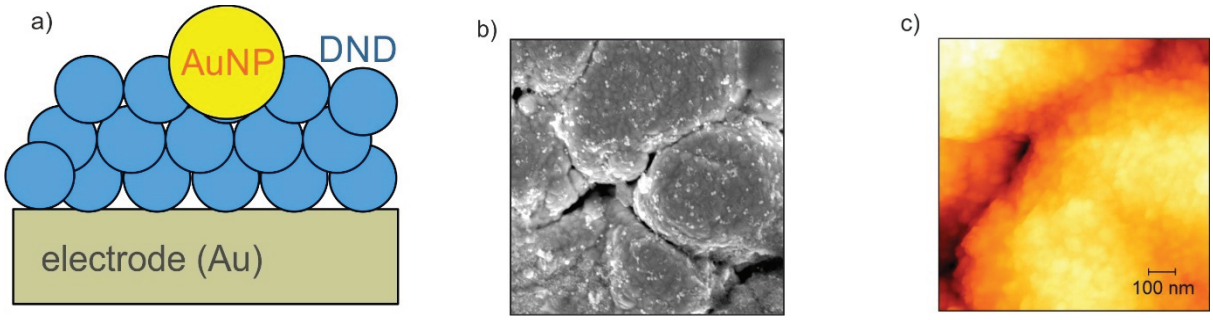

Figure 1a) Schematic cross-sectional drawing of the sensor coated with DND and AuNP, **b)** SEM morphology (2×2 um^2) of the sensor surface coated with O-DND/AuNP composite and with adsorbed drug, **c)** Detailed AFM topology (1×1 um^2) of the same surface

Figure 2 shows adhesion maps of the sensor coated with AuNP prior and after drug adhesion. Some rounded objects can be recognized on a smooth background in topography. Adhesion contrast reveals that they are different from the background and that they are composed of one to several rounded objects. Their height is about 20 nm. Their diameter is approximately 40 nm, however, that corresponds to 20 nm with AFM features being enlarged due to convolution with the tip of a typical diameter of 20 nm. Thus, these objects can be

attributed to our 20 nm gold nanoparticles. Typical adhesion values are around 1.4 nN for these AuNP and 1.9 nN for the background electrode.

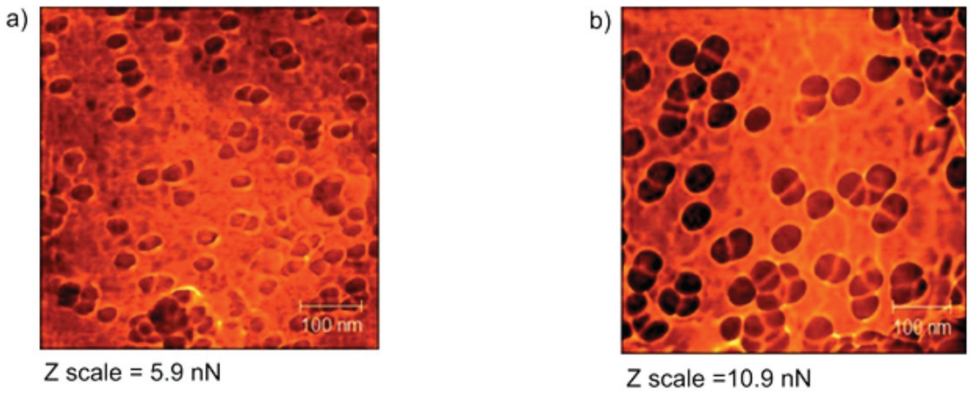

Figure 2 Detailed AFM surface adhesion maps of **a)** sensor coated with AuNP, **b)** sensor coated with AuNP after exposure to EN drug

Figure 2b shows that the drug absorption has a pronounced effect on the adhesion. Typical adhesion values are about 1.7 nN for AuNP and 3.2 nN for the electrode. This is a change of approximately 50 %. Importantly, adhesion on both AuNP and electrode change, hence the drug binds to both electrode and AuNP.

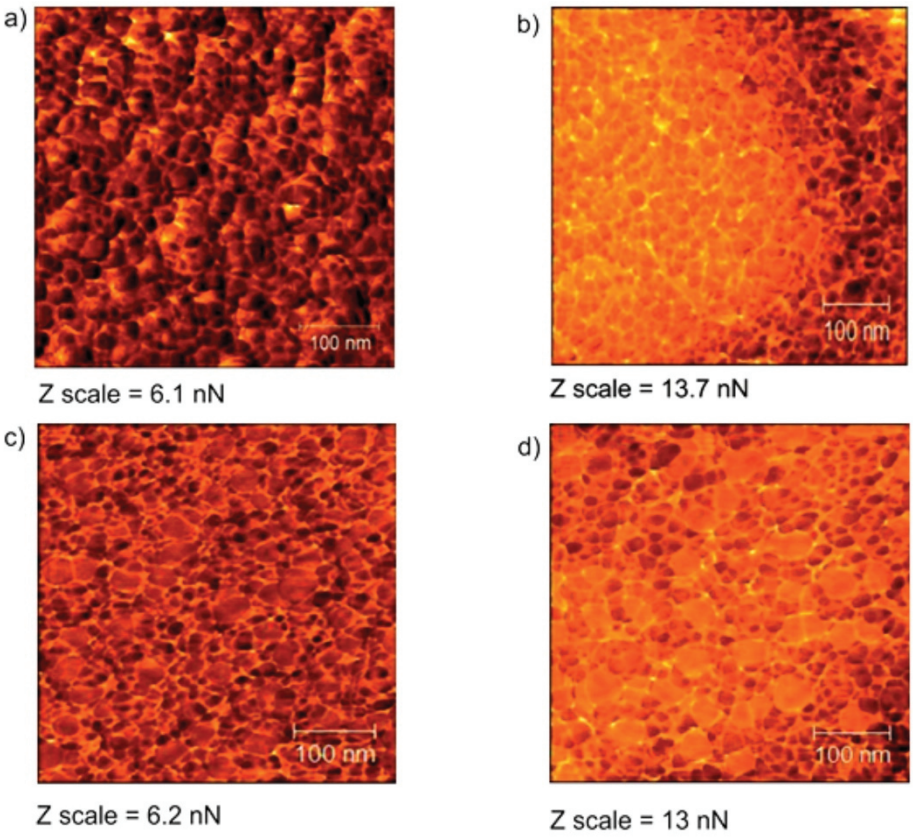

Figure 3 Detailed AFM surface adhesion maps of **a)** sensor coated with H-DND, **b)** sensor coated with H-DND after exposure to EN drug, **c)** sensor coated with H-DND/AuNP, **d)** sensor coated with H-DND/AuNP after exposure to EN drug

From adhesion map on the sensor coated with H-DND (**Figure 3a**) one can recognize a highly nanostructured surface morphology that is different to flat electrode background observed in **Figure 2**. There is a dense coverage by many small particles down to about 5 nm in size. It is thus obvious that the sensor surface is densely covered by H-DND. Typical adhesion values are around 1.8 nN on the H-DND nanoparticles and 3.3 nN on the electrode (measured in a small pinhole). After absorption of the drug (**Figure 3b**), the adhesion increased to 5.3 nN on the H-DND nanoparticles and to 7.4 nN on the electrode. The root mean square (RMS) of adhesion is around 0.5 nN in both cases, thus the difference is significant.

On the surface of a sensor where AuNP is added to H-DND (**Figure 3c**) one can recognize larger brighter particles among the smaller darker particles in the adhesion map. Considering the results on AuNP in **Figure 2**, these features can be attributed to the AuNP embedded in the H-DND layer. Typical adhesion values are about 1.4 nN on Au nanoparticles and 0.7 nN on the H-DND. Adhesion map on the H-DND/AuNP sensor after drug exposure (**Figure 3d**) shows an increase in adhesion. Typical adhesion on AuNP is 5.8 nN and on H-DND it is 3.3. nN. This is 320 % increase in adhesion. The drug again binds to both AuNPs and H-DNDs.

Figure 4 shows adhesion maps of the sensors coated with O-DND nanoparticles. Most of the surface is covered by O-DND nanoparticles. Typical adhesion on O-DND particles is 1.9 nN and on background electrode is 6.7 nN (measured in a pinhole). The drug adsorption reduces adhesion on O-DND. After drug exposure, typical adhesion value on O-DND particles is 0.8 nN and on the electrode it is 2.4 nN.

In the case of sensor coated with composite of O-DND/AuNP (**Figure 4 c-d**) AuNPs can be again recognized in the adhesion maps. Typical adhesion values on Au particles is 6.3 nN and on O-DND nanoparticles it is 9.9 nN. Adhesion after drug absorption decreases coated with composide O-DND/AuNP. Typical adhesion on Au particles is 4.2 nN and on O-DND nanoparticles is 2.4. nN.

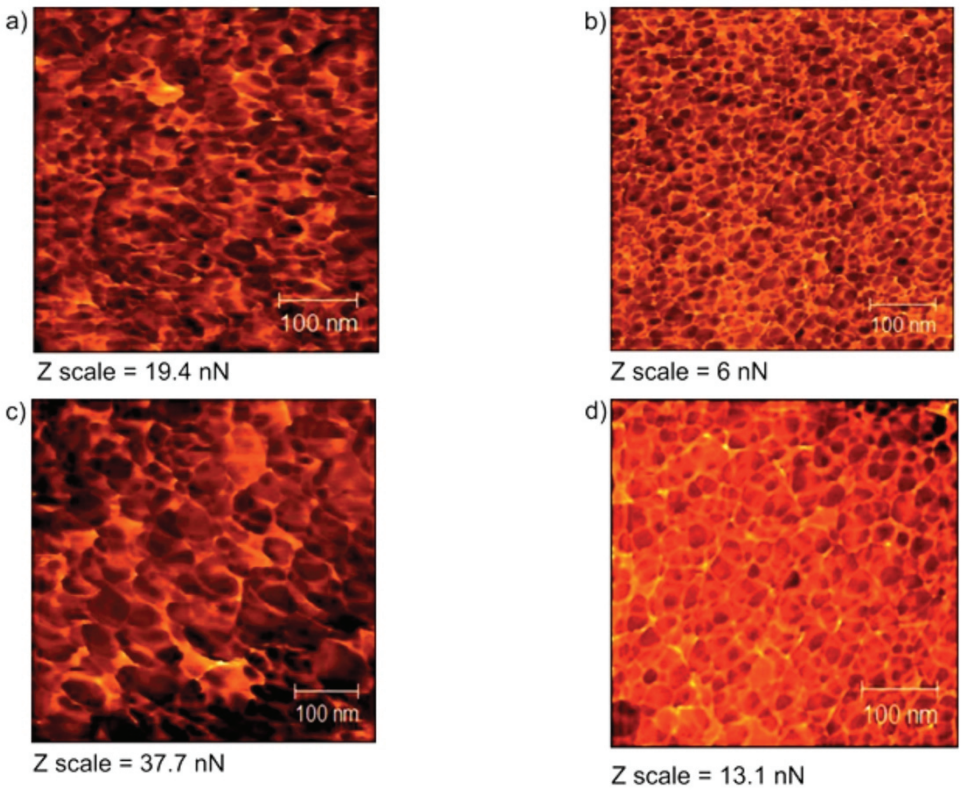

Figure 4 Detailed AFM surface adhesion maps of **a)** sensor coated with O-DND, **b)** sensor coated with O-DND after exposure to EN drug, **c)** sensor coated with O-DND/AuNP, **d)** sensor coated with O-DND/AuNP after exposure to EN drug

All values of adhesion, on original and drug exposed sensors are summarized in graph in **Figure 5**. It is evident that in the case of sensors coated with H-DND, drug 1-EN-142 increases adhesion, whereas on sensors coated with O-DND the drug decreases adhesion. The reproducible and consistent decrease of adhesion on O-DND based coatings compared to increase of adhesion on H-DND based coatings after drug exposure indicates different drug binding and conformation on these two nanomaterials.

In addition, H-DND and O-DND have also impact on the way how the drug binds to AuNP. Noticeably, after drug adsorption the adhesion on AuNP that is embedded in H-DND layer is 5× larger than on AuNP alone (see **Figure 2b**). Similarly this happens on AuNP that is embedded in O-DND, but the effect has opposite direction, the adhesion decreases after the drug adsorption. Noticeably, AuNP on O-DND exhibits much higher adhesion forces already before drug exposure.

The difference is most likely related to different AuNP charges when interacting with different substrates [7]. This is supported by the observation that the presence of H-DND also increased the density of deposited Au nanoparticles compared to other substrates. Different drug-adhesion responses on the same material can be thus observed with different substrates.

There is also different adhesion on H-DND or O-DND when alone or combined with AuNP. While the nanoparticles, coating process, and the sensor substrate are the same, the most likely explanation is change of nanodiamond surface due to exposure to AuNP colloidal solution containing citrates.

Different adhesion is observed also on background electrode when measured on different sensors. However, the free electrode area is small on coated sensors. Thus the adhesion is influenced not only by the interaction of the tip with the electrode but also with the nanoparticles on tip sides. The situation is schematically illustrated by the inset in **Figure 5**. Due to this effect the adhesion and its change after drug adsorption is the same as for given nanoparticle coating. In other words, due to sideway interaction of the tip with the nanoparticles the observed adhesion is not really controlled by the bottom electrode.

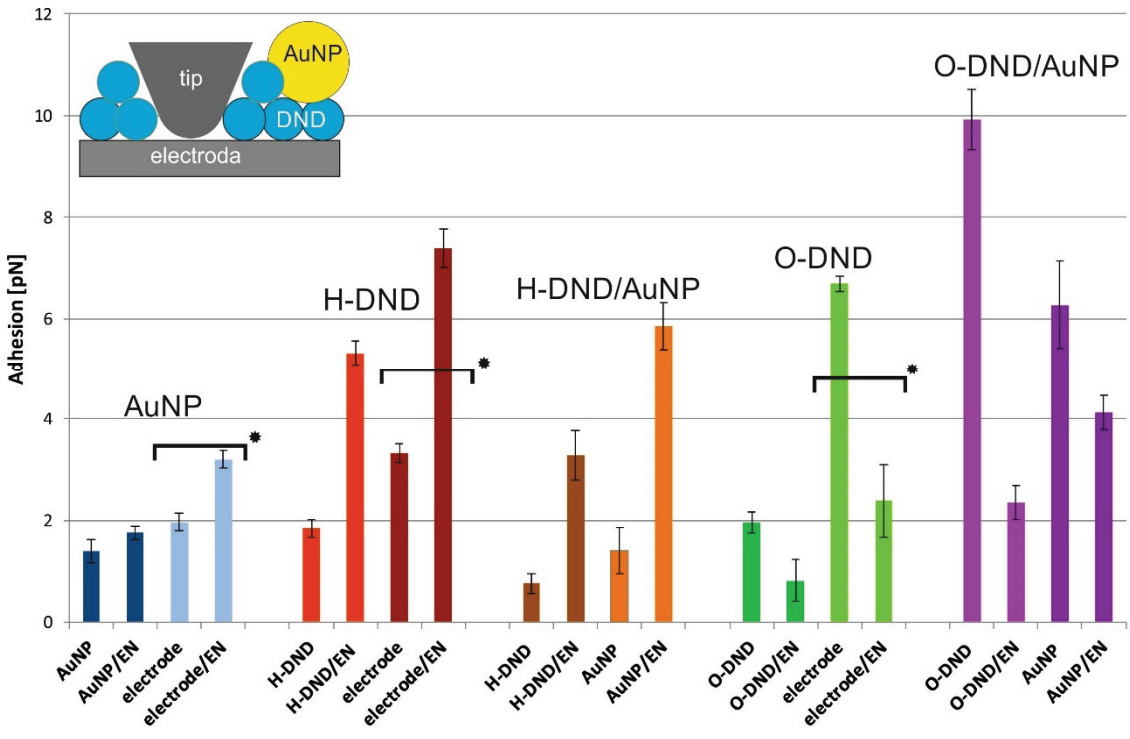

Figure 5 Bar graph of adhesion on individual particles on sensors with various nanoparticle coating.
***** Adhesion when tip interacts with bottom electrode. The inset shows schematic drawing of such interaction.

4. CONCLUSION

We combined 5 nm nanodiamond coatings with 20 nm gold nanoparticles to create functional coatings on impedance sensor substrates. The microscopic morphology of the coatings was characterized by SEM and AFM, revealing nanoscale composite formation with uniformly distributed AuNP. The obtained adhesion maps from AFM showed that 1-EN-142 Alzheimer drug binds to all nanoparticle materials (DND-H, O-DND, AuNP). The drug binds to these nanoparticles whether they are standalone or combined in the composite. However, it binds in different configurations as indicated by opposite adhesion change on H-DND and O-DND based coatings. Interestingly the adhesion on AuNP depends significantly on surrounding materials, most likely due to different nanoparticle charging. The study thus may help understand biosensor response.

ACKNOWLEDGEMENTS

The work has been supported by the GACR project 17-19968S.

REFERENCES

[1] ZHANG, Wenli, Kush PATEL, Andrew SCHEXNIDER, Shirin BANU a Adarsh D. RADADIA. Nanostructuring of Biosensing Electrodes with Nanodiamonds for Antibody Immobilization. ACS Nano 2014, 8(2), 1419-1428 DOI: 10.1021/nn405240g. ISSN 1936-0851.

[2] CAI, Weibo. Applications of gold nanoparticles in cancer nanotechnology. Nanotechnology, Science and Applications [online]. 2008, 1, 17-32. DOI: 10.2147/NSA.S3788. ISSN 1177-8903.

[3] J.A. Carlisle, Diamond films: Precious biosensors, Nat. Mater. 3 (2004) 668-669. DOI:10.1038/nmat1225.

[4] STEINMULLERNETHL, D, F KLOSS, M NAJAMULHAQ, et al. Strong binding of bioactive BMP-2 to nanocrystalline diamond by physisorption. Biomaterials. 2006, 27(26), 4547-4556. DOI: 10.1016/j.biomaterials.2006.04.036. ISSN 01429612. .

[5] M. Krátká, A. Kromka, E. Ukraintsev, M. Ledinský, A. Brož, M. Kalbacova, B. Rezek, Function of thin film nanocrystalline diamond-protein SGFET independent of grain size, Sens. Actuators B Chem. 166-167 (2012) 239-245. doi:10.1016/j.snb.2012.02

[6] NEPOVIMOVA, Eugenie, Elisa ULIASSI, Jan KORABECNY, et al. Multitarget Drug Design Strategy: Quinone-Tacrine Hybrids Designed To Block Amyloid-β Aggregation and To Exert Anticholinesterase and Antioxidant Effects. Journal of Medicinal Chemistry. 2014, 57(20), 8576-8589 DOI: 10.1021/jm5010804. ISSN 0022-2623.

[7] STEHLIK, Stepan, Tristan PETIT, Hugues A. GIRARD, Alexander KROMKA, Jean-Charles ARNAULT a Bohuslav REZEK. Surface potential of diamond and gold nanoparticles can be locally switched by surrounding materials or applied voltage. Journal of Nanoparticle Research [online]. 2014, 16(4),. DOI: 10.1007/s11051-014-2364-8. ISSN 1388-0764.

[8] NEČAS, David a Petr KLAPETEK. Gwyddion: an open-source software for SPM data analysis. Open Physics [online]. 2012, 10(1) [cit. 2018-10-17]. DOI: 10.2478/s11534-011-0096-2. ISSN 2391-5471. Dostupné z: http://www.degruyter.com/view/j/phys.2012.10.issue-1/s11534-011-0096-2/s11534-011-0096-2.xml

[9] GAN, Yang. Atomic and subnanometer resolution in ambient conditions by atomic force microscopy. Surface Science Reports. 2009, 64(3), 99-121. DOI: 10.1016/j.surfrep.2008.12.001. ISSN 01675729.